X International Conference on Computational Methods for Coupled Problems in Science and Engineering
COUPLED PROBLEMS 2023
M. Papadrakakis, B. Schrefler and E. Oñate (Eds)

ON NUMERICAL SIMULATION OF FLUID - STRUCTURE-ACOUSTIC INTERACTIONS RELATED TO HUMAN PHONATION PROCESS

P. SVÁČEK*, J. VALÁŠEK*,† AND K. VACEK*,†

*Czech Technical University in Prague
Faculty of Mechanical Engineering, Department of Technical Mathematics
Karlovo nám. 13, Praha 2, Czech Republic
e-mail: petr.svacek@fs.cvut.cz

†Institute of Mathematics, Czech Academy of Sciences

Key words: finite element method, phonation, fluid-structure-acoustic interactions

Abstract. This paper focus on mathematical modelling and numerical simulation of human phonation process. The mathematical FSI model is presented consisting of the description of the structural model, the flow model and the coupling conditions. In order to treat the VFs contact, the problem of the glottis closure is addressed. To this end several ingredients are used including the use of suitable boundary conditions, modification of the flow model and robust mesh deformation algorithm. The FSI model is extended to FSAI problem by inclusion of the Lighthill model of aeroacoustics. The numerical approximation of the problem is presented and several numerical results are shown.

1 INTRODUCTION

Mathematical models of fluid-structure interaction (FSI) problems and their numerical simulations are in last decades becoming more important in large variaty of applications. Recently, except the aerospace, civil and mechanical engineering applications, see e.g. [4], also the numerical methods for solution of FSI problems are being developed also in the field of biomechanics, [5]. In particular let us mention the biomechanics of voice, where the methods of numerical simulation of human phonation process are currently in an intensive development, see [22]. During the phonation the fundamental sound is created by vibrations of vocal folds induced by the airflow coming from the human lungs. This primary sound is further modulated by the geometry of the vocal tract corresponding to a pronounced vowel, see e.g. [7].

Although the air flow is compressible for the purpose of simulations the incompressible model is used justified by the fact that the maximal flow velocities in the vocal tract during phonation are well bellow 90 m/s. This peak of maximal velocity is occuring only in the glottis area, whereas the typical flow velocities in the other areas are significantly smaller. The compressible effects are modelled using an aeroacoustic analogy. Such approach is usually referred to as hybrid approach, see e.g. [21].

In this paper we are concerned with the fluid-structure-acoustic interaction problem consisting of the interaction of incompressible flow and a nonlinear elastic structure in 3D. The mutual

interaction is then coupled to the acoustic problem. The problem is mathematically described and numerically approximated.

Further attention is paid to the problem of treatment of the periodical closure of the glottal area. Here, the approach proposed in [18, 17] is extended to the more general situation of elastic structure. The paper is structured into this introduction followed by mathematical description of the FSAI problem. Section 3 is devoted to the numerical approximation of the problem, section 4 then presents numerical results obtained by the in-house developed code namely for the three dimensional problems.

2 MATHEMATICAL DESCRIPTION

2.1 Structural model

In this section the problem of deformation of an hyperelastic structure is described mathematically. Let us consider elastic structure represented by a *material* or reference configuration, a bounded domain $\Omega^s \subset \mathbb{R}^3$ with the Lipschitz continuous boundary $\partial\Omega^s$. The elastic body is deformed and its deformation is denoted by $\varphi : \overline{\Omega} \times [0,T] \to \mathbb{R}^3$, where φ is supposed to be orientation preserving bijection of Ω onto $\Omega^{\varphi_t} = \varphi(\Omega, t)$. For the stationary case the time variable t is omitted in what follows, i.e. $\Omega^\varphi = \Omega^{\varphi(t)}$. Here, Ω^φ is called the *actual* configuration and the mapping φ is called the deformation. It maps a material point x to the point in actual configuration x^φ given as $x^\varphi = \varphi(x)$, or $x^\varphi = \varphi(x,t)$. The deformation can be described with the aid of the displacement function

$$\varphi(x,t) = x + \boldsymbol{u}(x,t) \quad \text{for } x \in \Omega, t \in [0,T].$$

In what follows the following notation is used, $\boldsymbol{F}$ is the deformation gradient, $\boldsymbol{C}$ is the right Cauchy-Green tensor and by $\boldsymbol{E}$ the Green strain tensor is denoted

$$\boldsymbol{F} = \nabla\varphi(x) = \boldsymbol{I} + \nabla\boldsymbol{u}, \quad \boldsymbol{C} = \boldsymbol{F}^T\boldsymbol{F}, \quad \boldsymbol{E} = \frac{1}{2}(\boldsymbol{C} - \boldsymbol{I}) \tag{1}$$

where the Green strain tensor is given as

$$\boldsymbol{E} = \frac{1}{2}(\nabla\boldsymbol{u} + \nabla^T\boldsymbol{u}) + \frac{1}{2}\nabla^T\boldsymbol{u}\nabla\boldsymbol{u}, \qquad E_{ij} = \frac{1}{2}\left(\frac{\partial u_i}{\partial x_j} + \frac{\partial u_j}{\partial x_i}\right) + \frac{1}{2}\frac{\partial u_k}{\partial x_i}\frac{\partial u_k}{\partial x_j}. \tag{2}$$

The governing equations of elastic structure motion are the balance equa- tions in the deformed domain $\Omega^{\varphi,t}$

$$\rho^\varphi \frac{D^2\boldsymbol{u}}{Dt^2} - \nabla\cdot\boldsymbol{\sigma}^\varphi = \boldsymbol{g}^\varphi, \tag{3}$$

where $\frac{D}{Dt}$ denotes the material derivative, ρ^φ denotes the density of the material, $\boldsymbol{g}^\varphi$ represents the volume forces acting on the structure, $\boldsymbol{\sigma}^\varphi$ is the Cauchy stress tensor.

As the deformed domain $\Omega^{\varphi,t}$ depends on the displacement $\boldsymbol{u}$, it is suitable to rewrite the equations in the reference(material) domain Ω^s. In this case the equations to be solved are given in Ω^s as

$$\rho^s \frac{D^2\boldsymbol{u}}{Dt^2} - \nabla\cdot\boldsymbol{\Sigma}^s = \boldsymbol{g}, \tag{4}$$

where ρ^s denotes the density of the material given in the reference domain, $\boldsymbol{\Sigma}^s$ is the first Piola-Kirchoff tensor related to the Cauchy stress tensor by $\boldsymbol{\Sigma}^s = J\boldsymbol{\sigma}^\varphi\mathbb{F}^{-T}$. For the Cauchy

stress tensor it is neccessary to provide a constitutive relation, which is usually expressed in terms of the symmetric second Piola-Kirchhoff tensor $\boldsymbol{S}^s$, which is given by

$$\boldsymbol{S}^s = \mathbb{F}^{-1}\boldsymbol{\Sigma}^s = J\mathbb{F}^{-1}\boldsymbol{\sigma}^{\varphi}\mathbb{F}^{-T} \tag{5}$$

In this paper the St.Venant-Kirchhoff material model is used as an example of hyperelastic isotropic material. For the St.Venant-Kirchhoff model the constitutive relation is given

$$\boldsymbol{S}^s = \lambda^s(\mathrm{tr}\,\boldsymbol{E})\mathbb{I} + 2\mu^s\boldsymbol{E}, \tag{6}$$

where λ^s and μ^s denotes the Lamé coefficients related to the Young modulus E and Poisson ratio ν^s.

System of equations (4) is equipped with an initial condition for $\boldsymbol{u}$ and for $\frac{\partial \boldsymbol{u}}{\partial t}$, and with mixed boundary conditions. The homogenous Dirichlet boundary condition is used everywhere except at the interface with the fluid domain, where the boundary condition is specified by

$$\boldsymbol{\sigma}^{\varphi}\cdot\boldsymbol{n} = \boldsymbol{T}^S \qquad \text{on } \Gamma^{\varphi}_{Wt}, \tag{7}$$

where $\boldsymbol{T}^S$ denotes the aerodynamic forces acting on the structure determined by the solution of the flow model.

2.2 Flow model

First, let us emphasize that the moving structure results in the time dependent fluid domain Ω^f_t. In particular the motion of the interface Γ_{Wt} - i.e. the part of the fluid domain boundary which corresponds to the surface of the structure neighbouring the fluid domain - needs to be treated. The two-dimensional flow motion is described using the incompressible Navier-Stokes equations in the ALE conservative form, cf. [12]. Let us assume that for any $t \in (0,T)$ there exists (smooth enough) bijection of the reference configuration $\overline{\Omega}^f_0$ onto $\overline{\Omega}^f_t$, i.e. the so-called ALE mapping $\mathcal{A}_t : \overline{\Omega}^f_0 \to \overline{\Omega}^f_t$. The ALE conservative form of the Navier-Stokes equations reads

$$\begin{aligned} \frac{1}{\mathcal{J}_{\mathcal{A}}}\frac{D^{\mathcal{A}_t}}{Dt}\Big(\mathcal{J}_{\mathcal{A}}\boldsymbol{v}\Big) + \nabla\cdot((\boldsymbol{v}-\boldsymbol{w}_D)\otimes\boldsymbol{v}) &= \frac{1}{\rho^f}\nabla\cdot\boldsymbol{\tau} + \boldsymbol{f} \quad \text{in } \Omega_t \\ \nabla\cdot\boldsymbol{v} &= 0 \end{aligned} \tag{8}$$

where $\boldsymbol{v}$ is the flow velocity, symbol $D^{\mathcal{A}_t}/Dt$ denotes the ALE derivative (i.e. the time derivative with respect to the reference configuration, see e.g. [13]), $\boldsymbol{w}_D$ denotes the domain velocity, ρ^f denotes the constant fluid density, $\mathcal{J}_{\mathcal{A}}$ denotes the Jacobian of the ALE mapping and $\boldsymbol{\tau}$ is the Cauchy stress tensor given by

$$\boldsymbol{\tau} = -p\mathbb{I} + \mu\left(\nabla\boldsymbol{v} + \nabla^T\boldsymbol{v}\right), \quad \tau_{ij} = \left[-p\delta_{ij} + \mu\left(\frac{\partial v_i}{\partial x_j} + \frac{\partial v_j}{\partial x_i}\right)\right], \tag{9}$$

where p is the pressure, μ is the viscosity and δ_{ij} is the Kronecker's delta.

System of equations (8) is equipped with an initial condition

$$\boldsymbol{v}(x,0) = \boldsymbol{v}_0(x) \qquad x \in \Omega^f_0, \tag{10}$$

and by mixed boundary conditions. In order to specify the boundary conditions the boundary $\partial\Omega$ of the computational domain Ω is decomposed into the inlet Γ_I, the interface Γ_{Wt} and the outlet Γ_O, i.e. $\partial\Omega = \Gamma_{Wt} \cup \Gamma_O \cup \Gamma_I$. The following boundary conditions are used

$$\begin{aligned}
&\text{a)} -\nu\frac{\partial \boldsymbol{v}}{\partial \boldsymbol{n}} + (p - p^I_{ref})\boldsymbol{n} - \frac{1}{2}(\boldsymbol{v}\cdot\boldsymbol{n})^- \boldsymbol{v} &&= \frac{1}{\varepsilon}(\boldsymbol{v} - \boldsymbol{v}_D), && x \in \Gamma_I, t \in (0,T)\\
&\text{b)} \boldsymbol{v}(x,t) &&= \boldsymbol{w}_D(x,t) && x \in \Gamma_{Wt}, t \in (0,T)\\
&\text{c)} -\nu\frac{\partial \boldsymbol{v}}{\partial \boldsymbol{n}} + (p - p_{ref})\boldsymbol{n} - \frac{1}{2}(\boldsymbol{v}\cdot\boldsymbol{n})^- \boldsymbol{v} &&= 0, && x \in \Gamma_O, t \in (0,T).
\end{aligned} \tag{11}$$

2.3 Coupled problem

The fluid model (8) and the structural model (4) are coupled by two explicit conditions. First, the kinematic boundary condition (11b) prescribed at the surface Γ_{Wt}, where the domain velocity is equal to the structural velocity, i.e. $\boldsymbol{w}_D = \frac{D\boldsymbol{u}}{Dt}$.

The second coupling condition is the dynamic boundary conditions represented by the boundary condition (7 b), where the vector $\boldsymbol{T}^s$ is given as

$$\boldsymbol{T}^s \boldsymbol{\tau}^f \cdot \boldsymbol{n}. \tag{12}$$

with the fluid stress tensor $\boldsymbol{\tau}^f$ given by (9).

Last, both problems are moreover coupled due to the deformation of the domain Ω^f_t, which surrounds the vibrating surfaces of the elastic bodies Ω^s_t. The ALE mapping $\mathcal{A}_t$ can be considered as a smooth extension of the Lagrangian mapping from Ω^s_{ref} onto the domain $\Omega_{ref} = \Omega^s_{ref} \cup \Gamma_{W,ref} \cup \Omega^f_{ref}$. The ALE mapping $\mathcal{A}_t$ is described using an extension $\boldsymbol{u}^{ext}$ from $\overline{\Omega^s}$ onto $\overline{\Omega_{ref}}$ of the displacement $\boldsymbol{u}$ as

$$\mathcal{A}_t(X) = X + \boldsymbol{u}^{ext}(X,t) \tag{13}$$

for any $X \in \Omega^f_0$. This extension satisfy $\boldsymbol{u}^{ext}(x,t) = \boldsymbol{u}(x,t)$ for any $x \in \overline{\Omega^s_{ref}}$ and for any $t \in (0,T)$. The displacement $\boldsymbol{u}^{ext}$ can be written as a solution of an abstract boundary value problem, see e.g. [23] or [15].

2.4 Acoustics and Aeroacoustics

For modelling of sound propagation here either the acoustic model based on the Lighthill's analogy or other acoustic analogies are used, see [9], [20] or [14]. For the sake of brevity only the description of the Lighthill's analogy is shortly discussed here. The sound propagation is modelled in the acoustic domain Ω^a which contains a (smaller) subdomain Ω^f_t occupied by a flowing (compressible) fluid, whose flow is characterized by the velocity $\boldsymbol{u}$, the fluctuating pressure $p' = p - p_0$ and fluctuating density $\rho' = \rho - \rho_0$. For purpose of the acoustic problem the fluid domain Ω^f_t is assumed to be fixed, i.e. $\Omega^f_t \approx \Omega^f_0$ as well as the whole acoustic domain Ω^a. The fluid in the acoustic domain Ω^a except Ω^f_0 is assumed to be at rest with the mean density ρ_0, the mean pressure p_0 and the speed of sound c_0.

The acoustic analogy is derived using the momentum conservation, the assumption of the isentropic flow and the continuity equation, , see [9]. This leads to the wave equation for the unknown pressure fluctuation $p' = p - p_0$ given as $\frac{1}{c_0^2}\frac{\partial^2 p'}{\partial t^2} - \Delta p' = 0$, which describes the sound propagation in the domain Ω^a except the fluid domain, where the aeroacoustics sources needs

to be considered. Using the same procedure the inhomogeneous wave equation for the unknown pressure fluctuation $p' = p - p_0$ reads

$$\frac{1}{c_0^2}\frac{\partial^2 p'}{\partial t^2} - \Delta p' = \frac{\partial^2 T_{ij}}{\partial x_i \partial x_j}, \tag{14}$$

where on the right hand side a term describing the sound sources appears given by the so-called Lighthill tensor T_{ij} where the approximation for low Mach number flows is used

$$T_{ij} \approx \rho_0 v_i v_j, \tag{15}$$

see [10]. Equation 14 is equipped with the sound hard boundary condition prescribed at the channel walls, the sound emitting condition is used on the part corresponding to the vibrating surface of the vocal folds and the Sommerfeld boundary condition is used at the free field part of the boundary, see e.g. [10]. The latter condition can be replaced alternatively by the perfectly matched layer(PML) approach, see [20].

2.5 Glottis closure model

Several simplifications are used in order to address the closure of the glottis. First, only the symmetric two-dimensional motion of the vocal folds is assumed and consequently the computational domain Ω_t^f is assumed to be symmetric, see Figure 1, where at the axis of symmetry the symmetry boundary condition is prescribed. Further, only a simplified model is used for the structure depending on two degrees of freedom similarly as in [16]. This is justified as the dynamic mode decomposition of the motion during the phonation showed that there are only a small limited number (2-3) of shapes involved, which well corresponds to the eigenmodes of the structure.

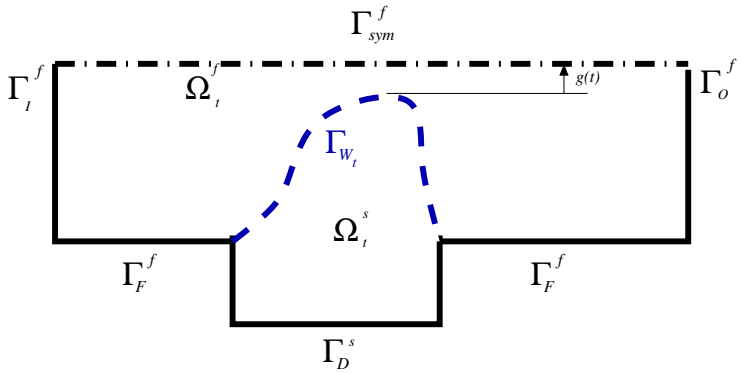

Figure 1: Computational domain for the FSI problem using the symmetry assumption for the purpose of application of glottis closure model

The presented mathematical model is an extension of the procedure proposed in [18] and consists of several ingredients. One of the ingredients is the already mentioned inlet boundary condition (11b), where the inlet flow velocity is prescribed using a penalization approach. Further, the modification of motion of the computational domain Ω_t^f during the closure phase needs to be applied. This modification is applied only for the closure phase, i.e. the case when

the half-gap $g(t)$ of the channel is bellow a given threshold g_{min}. The half-gap $g(t)$ is computed as (oriented) distance of the (lower part) vocal fold surface $\Gamma_{W,t}$ from the symmetry axis, see Fig. 1. Second, such a modification of Ω_t^f creates an artificial subdomain which should be occupied by the vocal fold. Here, the modified governing equations are used. Last, the contact in the structural domain needs to be considered. Here, only the model of Hertz's impact forces is discussed for the case of the simplified model.

Geometry modification For the open glottis phase, i.e. for $g(t) \geq g_{min}$, the computational domain Ω_t^f is kept unmodified. During the closure phase, i.e for the half gap $g(t) \leq g_{min}$, the displacement of the VF surface Γ_{Wt}^{VF} is modified in the fluid computational domain as Γ_{Wt}. This modification creates an artificial extension $\Omega_t^P \subset \Omega_t$ of the computational fluid domain, see Fig. 2. The domain Ω_t^P is determined as the part of domain which should be occupied by the VF.

Formally the set Ω_t^P is set empty, $\Omega_t^P = \emptyset$, for the opening phase. Similarly as in [18] we consider the geometrical modifications based on the local deformation of the surface only at the contact region, see Figure 2.

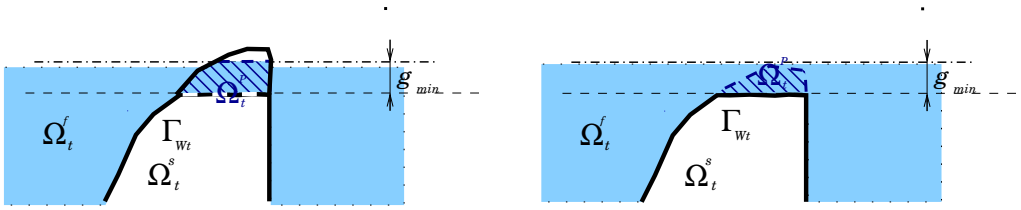

Figure 2: During the contact phase the geometry of the flow domain Ω_t^f does not fully follow the motion of the structure Ω_t^s but a subdomain of Ω_t^s is converted into the computational fluid domain as the porous media flow domain Ω_t^P. Such a modification is made not only in the closed case (on the left) but also in the case when then structure cross the artifical obstacle line (on the right).

Flow model modification The flow model is modified assuming that the subdomain Ω_t^P is domain of porous media with a given porosity. The flow model is then written with the aid of modified equations formally written in the whole computational domain Ω_t^f as

$$\frac{1}{\mathcal{J}_{\mathcal{A}}}\frac{D^{\mathcal{A}_t}}{Dt}\Big(\mathcal{J}_{\mathcal{A}}\boldsymbol{v}\Big) + \nabla\cdot((\boldsymbol{v}-\boldsymbol{w}_D)\otimes\boldsymbol{v}) + \boldsymbol{\sigma}_P(\boldsymbol{u}-\boldsymbol{w}_D) = \frac{1}{\rho^f}\nabla\cdot\boldsymbol{\tau} + \boldsymbol{f}, \qquad \nabla\cdot\boldsymbol{v} = 0$$

where $\boldsymbol{\sigma}_P = \sigma_P\chi_{\Omega_t^P}$, $\chi_{\Omega_t^P}$ is the indicator(characteristic) function of the set Ω_t^P and the coefficient $\sigma_P > 0$ corresponds to an artificial permeability of the fictitious porous media, see [2], or it can be understand as another penalization parameter, see [1].

Impact forces model During the contact phase the Hertz impact forces are used similarly as in [8] for the simplified problem. In this case the surface forces $\boldsymbol{T}^s$ in (7b) is modified by the addition of the Hertz impact force F_H which depends on the area of overlap of the elastic structure over the axis of symmetry. Here, a simplified model is used, where the Hertz impact

force is distributed to the forces $\boldsymbol{T}^s$ depending on the position x_{max} of the impact. The model of Hertz impact forces is given as $F_H = k_H \delta^{3/2}(1+b_H\dot{\delta})$ with $k_H \approx \frac{4}{3}\frac{E}{1-\mu_H^2}\sqrt{r}$, where δ stands for the penetration of the vocal fold through the contact plane (symmetry axis), b_H is a damping factor (here set to zero), r is the radius of the osculating circle (i.e. inverse of the curvature), E is Young's modulus of elasticity of the vocal fold and μ_H is its Poisson's ratio, for values see [8].

3 NUMERICAL APPROXIMATION

In this section the numerical approximation of the FSAI problem is described. First, we the problem is decoupled in the fluid, structural and acoustic part. For solution of each part the application of the finite element method is briefly described. Further, the coupling mechanism is shortly described.

3.1 Structural model

For the sake of brevity only the linear elasticity model is assumed here and its weak formulation is introduced in a standard way: the (linearized) problem (4) is multiplied by a test function $\boldsymbol{\psi} = (\psi^i)_i$ from the space of test functions $\boldsymbol{V} = \{\boldsymbol{\varphi} \in \boldsymbol{H}^1(\Omega^s) : \boldsymbol{\varphi}|_{\Gamma_D^s} = 0\}$, integrated over Ω^s, and with the use of Green's theorem and boundary condition (7b) we arrive to the weak formulation in the form

$$\left(\rho^s \frac{\partial^2 \boldsymbol{u}}{\partial t^2}, \boldsymbol{\psi}\right)_{\Omega^s} + (\boldsymbol{\tau}^s(\boldsymbol{u}), \boldsymbol{e}(\boldsymbol{\psi}))_{\Omega^s} = (\boldsymbol{f}^s, \boldsymbol{\psi})_{\Omega^s} + (\boldsymbol{T}^s, \boldsymbol{\psi})_{\Gamma_{W,0}}, \tag{16}$$

where by symbol $(\cdot,\cdot)_{\mathcal{M}}$ the dot product in the space $\boldsymbol{L}^2(\mathcal{M})$ is denoted. The approximate finite element solution of problem (16) sougth in the finite element subspace $\boldsymbol{V}_h \subset \boldsymbol{V}$, which is constructed with the aid of an admissible triangulation $\mathcal{T}_h^s$ of the computational domain Ω^s, see e.g. [3], i.e. in the space

$$\boldsymbol{V}_h = V_h^3, \quad V_h = \{\varphi \in C(\overline{\Omega^s}) : \varphi = 0 \text{ on } \Gamma_D^s, \varphi|_K \in P_1(K)\ \forall K \in \mathcal{T}_h^s\} \subset V, \tag{17}$$

where $P_1(K)$ is the space of polynomials of degree less or equal one on the triangle K. The finite element discretization leads to the system of ODEs

$$\mathbb{M}^s \ddot{\boldsymbol{U}} + \mathbb{D}^s \dot{\boldsymbol{U}} + \mathbb{K}^s \boldsymbol{U} = \boldsymbol{b}^s(t), \tag{18}$$

where $\boldsymbol{U} = \boldsymbol{U}(t)$ is the vector of unknowns, $\boldsymbol{b}^s(t)$ is the load vector, $\mathbb{M}^s$ is the mass matrix $\mathbb{M}^s = (m_{ij}^s)$, $\mathbb{K}^s$ is the stiffness matrix $\mathbb{K}^s = (k_{ij}^s)$. The term with the matrix $\mathbb{D}$ represents the (added) structural damping model based on the artificially added proportional damping $\mathbb{D} = \epsilon_1^s \mathbb{M} + \epsilon_2^s \mathbb{K}$ with suitably chosen parameters $\epsilon_1^s, \epsilon_2^s$.

3.2 Flow model

For the numerical approximation of the flow model (8) the problem is formulated weakly for the unknowns $U = (\boldsymbol{v}, p)$ leading to the equation valid for any test function $V = (\boldsymbol{\varphi}, q)$

$$\frac{d}{dt}\left[\left(\boldsymbol{v}, \boldsymbol{\varphi}\right)_{\Omega_t}\right] + \left(\boldsymbol{\tau}^f, \nabla\boldsymbol{\varphi}\right)_{\Omega_t} + c(\overline{\boldsymbol{w}}; \boldsymbol{v}, \boldsymbol{\varphi}) + \left(\nabla\boldsymbol{v}, q\right)_{\Omega_t} + \mathcal{B} = \left(\mathbf{f}, \boldsymbol{\varphi}\right)_{\Omega_t},$$

where $\overline{\boldsymbol{w}} := \boldsymbol{v} - \boldsymbol{w}_D$, c represents the skew-symmetric form of the convective term, and $\mathcal{B}$ represents several boundary terms depending on the prescribed boundary conditions, see [18]. Here, the test function $\boldsymbol{\varphi}$ is assumed to be constant with respect to the reference domain, i.e. $\frac{D^{\mathcal{A}}\boldsymbol{\varphi}}{Dt} \equiv 0$.

For the time discretization the same equidistant partition of the time interval with a constant time step Δt as for structure is used, i.e. $t_n = n\Delta t$, $\Delta t > 0$. The approximations of velocity $\boldsymbol{v}^n \approx \boldsymbol{u}(\cdot, t_n)$ and pressure $p^n \approx p(\cdot, t_n)$ are sought at time instants $t_n, n = 0, 1, \ldots,$ and an approximation of the domain velocity at time instant t_n is denoted by $\boldsymbol{w}_D^n$. For the time discretization the formally second order backward difference formula is used, i.e the time derivative in

$$\frac{d}{dt}\left[\Big(\boldsymbol{v}, \boldsymbol{\varphi}\Big)_{\Omega_t}\right] \approx \frac{1}{2\Delta t}\left[\Big(3\boldsymbol{v}^{n+1}, \boldsymbol{\varphi}\Big)_{\Omega_{t_{n+1}}} - \Big(4\boldsymbol{v}^{n}, \boldsymbol{\varphi}\Big)_{\Omega_{t_{n+1}}} + \Big(1\boldsymbol{v}^{n-1}, \boldsymbol{\varphi}\Big)_{\Omega_{t_{n+1}}}\right]. \tag{19}$$

The weak form of the time discretized problem is then stabilized using the fully stabilized scheme as describe in [6], modified for the purpose of the ALE mapping similarly as in [16], due to the used ALE conservative method and for the case of glottis closure, see [18]. The stabilized problem at time instant t_{n+1} form then reads: find finite element approximations $U = (\boldsymbol{u}, p) := (\boldsymbol{u}^{n+1}, p^{n+1})$ such that $\boldsymbol{u}$ satisfy the boundary condition (11b) and

$$a(U; U, V) + a_S(U; U, V) + \mathcal{P}_S(U, V) = L(V) + L_S(V) \tag{20}$$

holds for any test function $V = (\boldsymbol{\varphi}, q)$, where the terms $a(U; U, V)$ and $L(V)$ corresponds to the form (19) with the time discretization (19) used. The terms $a_S(U; U, V)$ and $L_S(V)$ corresponds to the SUPG/PSPG stabilization and $\mathcal{P}_S(U, V)$ represents the div-div stabilization, see [18].

3.3 Solution of coupled problem

Here, we focus only on description of the coupling of FSI problem. The coupling of acoustics with FSI is considered only one way, i.e. the acoustics depends on the computed flow field, but the influence of acoustics on the flow field and structural displacement is neglected.

During the computational process at any time instant t_n, $n = 1, 2, \ldots$ consists of finding the values of the velocity $\boldsymbol{v}^n$, the pressure p^n, the displacement $\boldsymbol{u}^n$ as well as its the first and the second derivatives $\dot{\boldsymbol{u}}^n$ and $\ddot{\boldsymbol{u}}^n$, respectively. Furthermore also the aerodynamical forces $(\boldsymbol{T}^s)_n$ and the ALE mapping $\mathcal{A}_{t_n}$ needs to be determine which describes the computational domain $\Omega_{t_n}^f$ as well as the domain velocity $\boldsymbol{w}_D^n$. The values for $n = 0$ at time instant t_0 are given by the specified initial condition.

Starting at time instant t_n we assume that all values are known. The solution procedure can be briefly described as the following steps

O. Approximate the aerodynamical forces $\boldsymbol{T}_{n+1}^s$ at t_{n+1} by extrapolation from the previous time steps.

I. Using the approximation of the aerodynamical forces $\boldsymbol{T}_{n+1}^s$ compute the displacement of the elastic domain $\boldsymbol{u}^{n+1}$ at time t_{n+1}.

II. Deform the computational domain $\Omega_{t_{n+1}}^f$ and construct the ALE mapping $A_{t_{n+1}}$ and ALE domain velocity $\boldsymbol{w}_D$ at time t_{n+1}.

III. Solve the fluid flow problem and determine the flow velocity $\boldsymbol{v}^{n+1}$ and the pressure p^{n+1}.

IV. Compute the aerodynamic forces acting on the structure.

V. Check whether the aerodynamic forces differs from the previous approximation $\boldsymbol{T}^s_{n+1}$: If **no**, set $n := n + 1$ and continue with the step **O.** If **yes**, use the newly computed aerodynamic forces $\boldsymbol{T}^s_{n+1}$ and with the step **I.**

3.4 Acoustics

The numerical approximation of the acoustic problem is performed in the standard way. The problem is weakly formulated and spatially discretized by the finite element method. For the aeroacoustics the Lighthill tensor is approximated by the convective part $T_{ij} \approx \rho_0 v_i v_j$, i.e. only the Lighthill analogy for low Mach number is considered. The acoustic pressure p' is approximated by the function p'_h at any time step from the standard scalar finite element space V_h of the piecewise linear functions. Such a approximation leads to the second order system of ODEs in the form

$$\frac{1}{c_0^2}\mathbb{M}^a \ddot{P} + \mathbb{K}^a P = \boldsymbol{b}^a(t), \tag{21}$$

where P denotes the vector of unknowns $\mathbb{M}^a$ and $\mathbb{K}^a$ denote the acoustic mass and the stiffness matrices, respectively, and the vector $\boldsymbol{b}^a(t)$ corresponds to the aeroacoustic source terms for the Lighthill analogy. The arising system of ODEs is numerically discretized in time by the classical Newmark method.

4 NUMERICAL RESULTS

4.1 Modal analysis

First, the natural modes of vibration inherent to the elastic vocal folds are investigated. Here, two models of vocal folds are considered. The first one corresponds to the reference [8], where the homogenous material is considered with Young modulus $E = 8kPa$, Poisson ratio $\mu = 0.4$ and the density $\rho^s = 1000\text{kg / m}^3$. The second model is more complicated model consisting of several layers of materials, see [24].

The first four eigenmodes and eigenfrequencies of the VF model MALE-SYM are shown in Figures 3. The first four lowest eigenfrequencies are $f_1 = 101.8159\,\text{Hz}$, $f_2 = 147.5051$, $f_3 = 160.3396$ and $f_4 = 175.3797$, where frequencies f_1 and $f_{3/4}$ are almost identical to the frequencies considered in article [16] (100 Hz and 160 Hz). Comparison of the eigenmodes in Figure 3 shows that the modes related to f_1 and f_3 well agrees with those determined in the two-dimensions. The mentioned frequencies corresponds well with the interval of the male VF vibration fundamental frequency $85 - 155$ Hz as published by [19]. Similar findings were obtained for the second VF model.

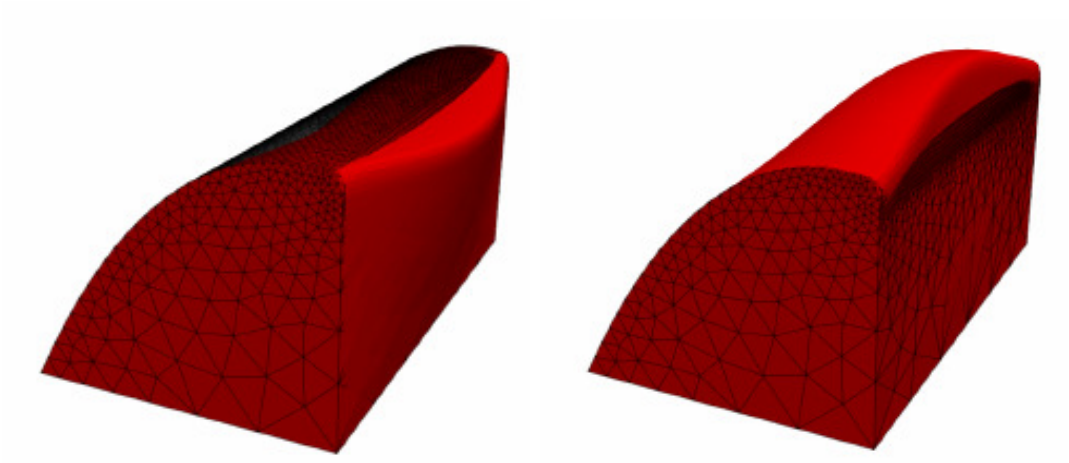

Figure 3: Eigenmodes of the structure corresponding to the eigenfrequencies f_1 and f_4.

4.2 Acoustic resonant frequencies of vocal tract

The sound created by the flow-induced vibration of VFs at the larynx propagates by the vocal tract (VT) to the mouth and further exterior. The characteristics of propagated sound is mostly influenced by the VT resonances. In the case of mathematical modelling these resonances can be significantly influenced also by the shape of the fluid flow domain Ω_t^f or by the shape of the connection of the flow domain to the acoustical domain. In order to analyze this influence several VT models are analyzed here in order to find their acoustic resonant frequencies, which are, in the human phonation context, usually called formants. Formants are usually characterized not only by the resonant frequency peak but also by the formants bandwidth, see [19].

The part of acoustic domain Ω_{tract}^a representing a VT model for the vowel [u:] is shown in Figure 4 together with the transfer function, where the formants were identified in the expected range.

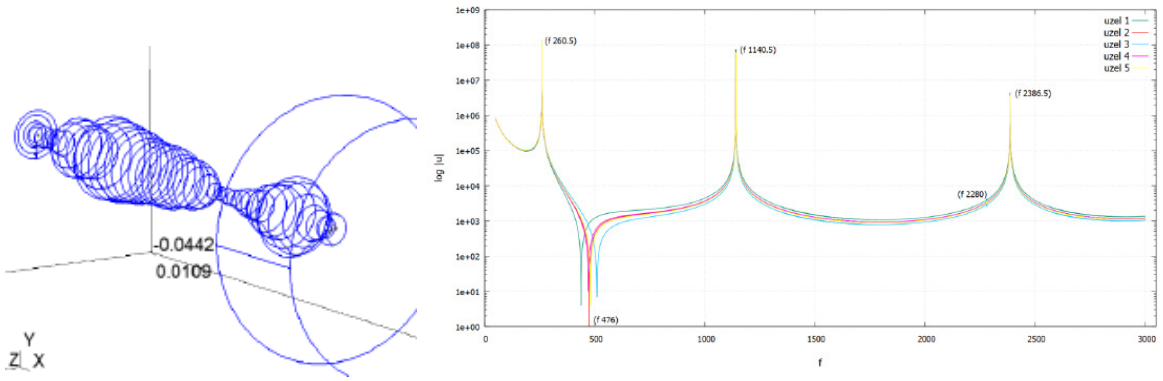

Figure 4: The geometry of the vocal tract and its formant detection using the transfer functions approach.

5 SUMMARY

In this paper the detailed mathematical model of the human phonation was introduced, where several phenomena was considered: namely the vibration of elastic vocal folds was treated

using the solution of hyperelastic problem, the air flow was described using the incompressible Navier Stokes equations and the Lighthill's acoustic analogy was used for treatment of the acoustic problem. The numerical approximation of the roblem was performed with the aid of the finite element method in space. The strongly coupled partitioned algorithm was used.

Acknowledgment The work was supported from European Regional Development Fund Project Center for Advanced Applied Science (No.CZ.02.1.01/0.0/0.0/16_019/0000778).

REFERENCES

[1] Ph Angot, Ch H Bruneau, and P Fabrie. A penalization method to take into account obstacles in incompressible viscous flows. *Numer Math*, 81, 1999.

[2] Burman, Erik, Fernández, Miguel A., and Frei, Stefan. A Nitsche-based formulation for fluid-structure interactions with contact. *ESAIM: M2AN*, 54(2):531–564, 2020.

[3] P. G. Ciarlet. *The Finite Element Methods for Elliptic Problems*. North-Holland Publishing, 1979.

[4] Earl H. Dowell and Robert N. Clark. *A modern course in aeroelasticity*. Solid mechanics and its applications. Kluwer Academic Publishers, Dordrecht, Boston, 2004.

[5] C.A. Figueroa, I.E. Vignon-Clementel, K.E. Jansen, T.J.R. Hughes, and C.A. Taylor. A coupled momentum method for modeling blood flow in three-dimensional deformable arteries. *Computational Methods in Applied Mechanical Engineering*, 195:5685–5706, 2006.

[6] T. Gelhard, G. Lube, M. A. Olshanskii, and J.-H. Starcke. Stabilized finite element schemes with LBB-stable elements for incompressible flows. *Journal of Computational and Applied Mathematics*, 177:243–267, 2005.

[7] J. Horáček, A. M. Laukkanen, P. Šidlof, P. Murphy, and J. G. Švec. Comparison of acceleration and impact stress as possible loading factors in phonation. A computer modeling study. *Folia Phoniatrica et Logopaedica*, 61(3):137–145, 2009.

[8] J. Horáček, P. Šidlof, and J. G. Švec. Numerical simulation of self-oscillations of human vocal folds with Hertz model of impact forces. *Journal of Fluids and Structures*, 20(6):853–869, 2005.

[9] M. S. Howe. *Theory of vortex sound*. Cambridge University Press, 2002.

[10] M. Kaltenbacher, S. Marburg, A. Beck, C.-D. Munz, U. Langer, and M. Neumüller. *Computational Acoustics*. Springer, 2018.

[11] M. J. Lighthill. On sound generated aerodynamically. I. General theory. In *Proceedings of the Royal Society of London*, volume 211, pages 564–587. The Royal Society, 1952.

[12] F. Nobile. *Numerical approximation of fluid-structure interaction problems with application to haemodynamics*. PhD thesis, Ecole Polytechnique Federale de Lausanne, 2001.

[13] T. Nomura and T. J. R. Hughes. An arbitrary Lagrangian-Eulerian finite element method for interaction of fluid and a rigid body. *Computer Methods in Applied Mechanics and Engineering*, 95:115–138, 1992.

[14] Stefan Schoder, Michael Weitz, Paul Maurerlehner, Alexander Hauser, Sebastian Falk, Stefan Kniesburges, Michael Döllinger, and Manfred Kaltenbacher. Hybrid aeroacoustic approach for the efficient numerical simulation of human phonation. *The Journal of the Acoustical Society of America*, 147, 1179, 2020. doi: 10.1121/10.0000785.

[15] P. Sváček. Numerical solution of fluid-structure interaction problems with considering of contacts. *Acta Polytechnica*, 61(SI):155–162, 2021.

[16] P. Sváček and J. Horáček. Numerical simulation of glottal flow in interaction with self oscillating vocal folds: comparison of finite element approximation with a simplified model. *Communications in Computational Physics*, 12(3):789–806, 2012.

[17] P. Sváček and J. Horáček. Finite element approximation of flow induced vibrations of human vocal folds model: Effects of inflow boundary conditions and the length of subglottal and supraglottal channel on phonation onset. *Applied Mathematics and Computation*, 319:178–194, 2018.

[18] P. Sváček and J. Horáček. FE numerical simulation of incompressible airflow in the glottal channel periodically closed by self-sustained vocal folds vibration. *Journal of Computational and Applied Mathematics*, 393:113529, 2021.

[19] Ingo R. Titze. *Principles of voice production*. Prentice-Hall Inc, 1993.

[20] J. Valášek, M. Kaltenbacher, and P. Sváček. On the application of acoustic analogies in the numerical simulation of human phonation process. *Flow Turbulence Combust*, 102:129–143, 2019.

[21] P. Šidlof, J. Horáček, and V. Řidký. Parallel CFD simulation of flow in a 3D model of vibrating human vocal folds. *Computers & Fluids*, 80:290–300, 2013.

[22] P. Šidlof, S. Zörner, and A Hüppe. A hybrid approach to computational aeroacoustics of human voice production. *Biomechanics and Modeling in Mechanobiology*, 14:473–488, 2015.

[23] Z. Yang and D. J. Mavriplis. Unstructured dynamic meshes with higher-order time integration schemes for the unsteady Navier-Stokes equations. In *43rd AIAA Aerospace Sciences Meeting*, page 13 pp., Reno NV, 2005. AIAA Paper 2005-1222.

[24] S. Zörner, M. Kaltenbacher, and M. Döllinger. Investigation of prescribed movement in fluid-structure interaction simulation for the human phonation process. *Computers & Fluids*, 86:133–140, 2013.